

Transition Intensities in the Local Mode Picture

Emil Vogt¹, Alexander Kjaersgaard¹, Lauri Halonen², and Henrik G. Kjaergaard¹

¹Department of Chemistry, University of Copenhagen, Universitetsparken 5, 2100 Copenhagen Ø, Denmark

²Department of Chemistry, University of Helsinki, P. O. Box 55 (A.I. Virtasen aukio 1), FI-00014, Finland.

The Local Mode Model

1) Find equilibrium geometries

We solve the electronic Schrödinger equation with *ab initio* methods to find the relevant conformers.

2) Local Mode (LM) Coordinates (q_1, q_2, \dots, q_M)

The q 's are defined based on the transitions of interest. Typically, vibrational modes that involve movement of the same atoms are included in the LM model. In practice, q 's are defined from the Z-matrix and one has to define a Z-matrix compatible the chosen q 's.

3) Potential Energy Surface (PES) and Dipole Moment Function (DMF)

In our calculations, the PES and DMF are typically truncated to only include pairwise coupling, i.e.

$$V(q_1, q_2, \dots, q_M) \approx \sum_i \left[V(q_i) + \sum_{j>i} V(q_i, q_j) \right]. \quad (1)$$

The 1D PESs ($V(q_i)$) are represented with spline fits and the 1D DMFs with sixth-order polynomials in the displacement coordinates for each Cartesian component. PES cross-terms ($V(q_i, q_j)$) and DMF cross-terms are expressed with 2D Taylor expansions in the respective displacement coordinates.

Molecular vibrational and rotational motion cannot be fully separated, but may be separated to the maximum extent if the rotational Eckart condition is satisfied. The rotational Eckart condition is

$$\sum_{a=1}^N m_a (\vec{R}_a \times \mathbf{U} \vec{r}_a) = \vec{0}, \quad (2)$$

where m_a is the mass of atom a , \vec{R}_a and \vec{r}_a are the radius-vectors of atom a in the equilibrium geometry and in the vibrationally distorted geometry, respectively, and \mathbf{U} is the rotation matrix that rotates \vec{r}_a to satisfy the rotational Eckart condition. We employ a numerical method^[1] to find \mathbf{U} and calculate each dipole moment single point in the Eckart frame

4) Calculate Wilson G-matrix elements

If not defined analytically, the elements of the G -matrix are calculated numerically from

$$\mathbf{G} = (\mathbf{J}^{-1})^T \mathbf{M}^{-1} \mathbf{J}^{-1}, \quad \text{with } J_{i\alpha} = \frac{\partial x_\alpha}{\partial q_i} \quad \& \quad M_{\alpha\beta} = m_\alpha \delta_{\alpha\beta}, \quad (3)$$

where $\alpha = 1, 2, \dots, 3N$ and x_1, x_2, x_3 are the x -, y - and z -coordinates of the first atom, x_4, x_5, x_6 are the x -, y - and z -coordinates of the second atom, etc. In practice, the Z-matrix is used to generate the change in all 3N-6 q 's and the Jacobian is then augmented with three rotational and three translational components.

5) Generate The M-Dimensional LM Hamiltonian

The LM Hamiltonian is obtained by transforming the nuclear Hamiltonian in Cartesian coordinates to internal curvilinear coordinates,

$$\hat{H} = -\frac{1}{2} \sum_{i,j} \hat{p}_i G(q_i, q_j) \hat{p}_j + V(q_1, q_2, \dots, q_M) + V', \quad (4)$$

where \hat{p} is the momentum operator and V' is the LM pseudopotential (often ignored). The LM Schrödinger equation is first solved for each mode and the full LM Hamiltonian is then set up in a product basis of the 1D eigenfunctions ($|v_1\rangle|v_2\rangle \dots |v_M\rangle$). The eigenvalues and eigenfunctions are obtained by diagonalizing the full LM Hamiltonian.

6) Calculate Transition Intensities

We express transition intensities in terms of dimensionless oscillator strengths

$$f_{i \rightarrow f} = 4.702 \cdot [\text{cm} \times \text{D}^{-2}] \tilde{\nu}_{i \rightarrow f} |\langle i | \hat{\mu} | f \rangle|^2, \quad (5)$$

where i and f are the initial and final states, $\tilde{\nu}_{i \rightarrow f}$ is the transition wavenumber in cm^{-1} and $|\langle i | \hat{\mu} | f \rangle|$ is the transition dipole moment expressed in Debye (D).

The OH-Stretch in 1-Propanol

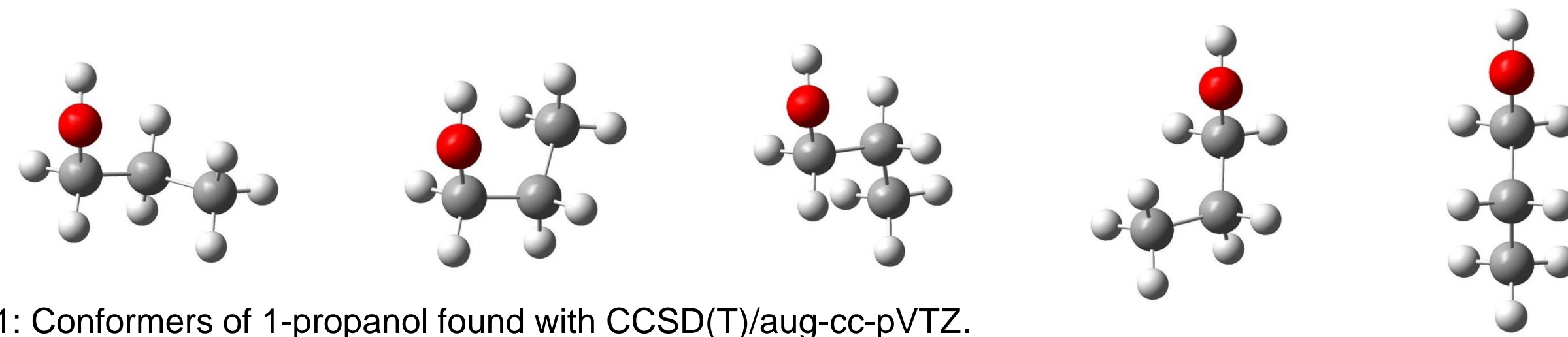


Figure 1: Conformers of 1-propanol found with CCSD(T)/aug-cc-pVTZ.

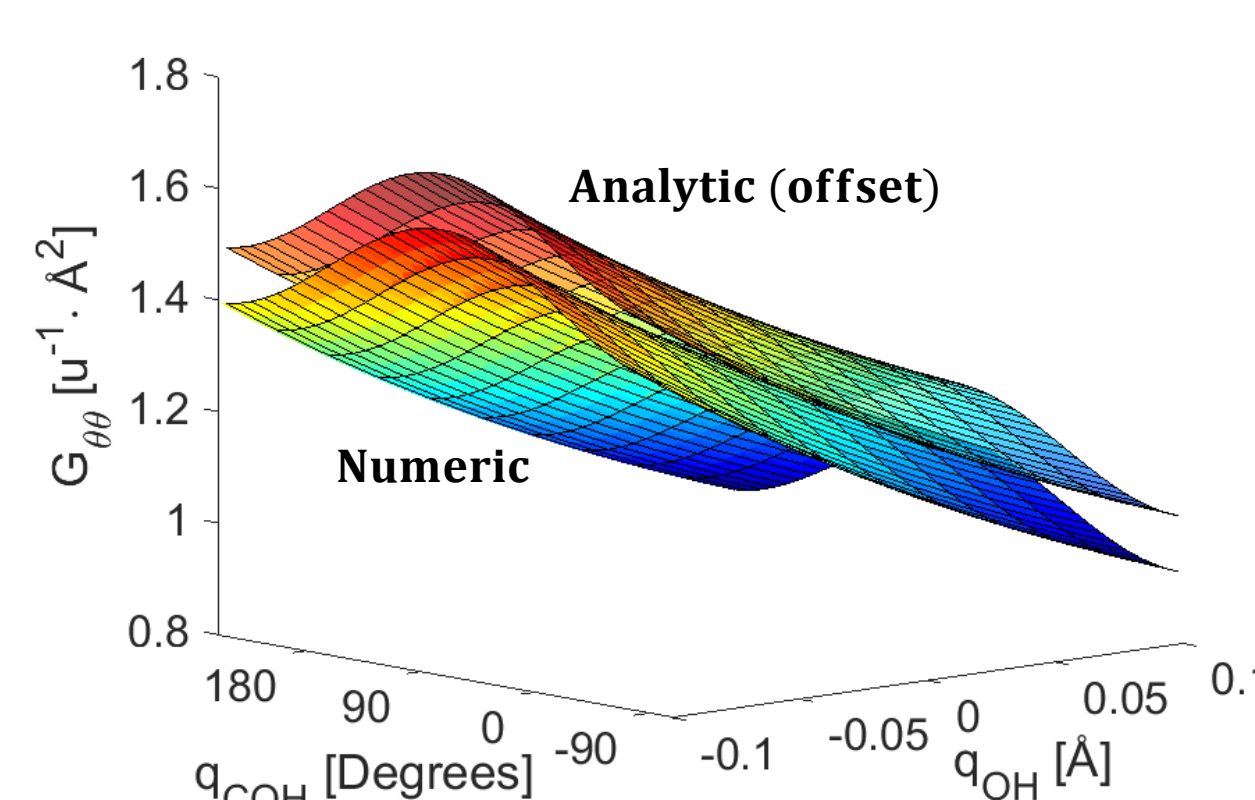


Figure 2: Numeric and analytical G-matrix element for the COH-bending mode in Gg-1-propanol. The analytical G-matrix element has been slightly offset to allow for a visual comparison.

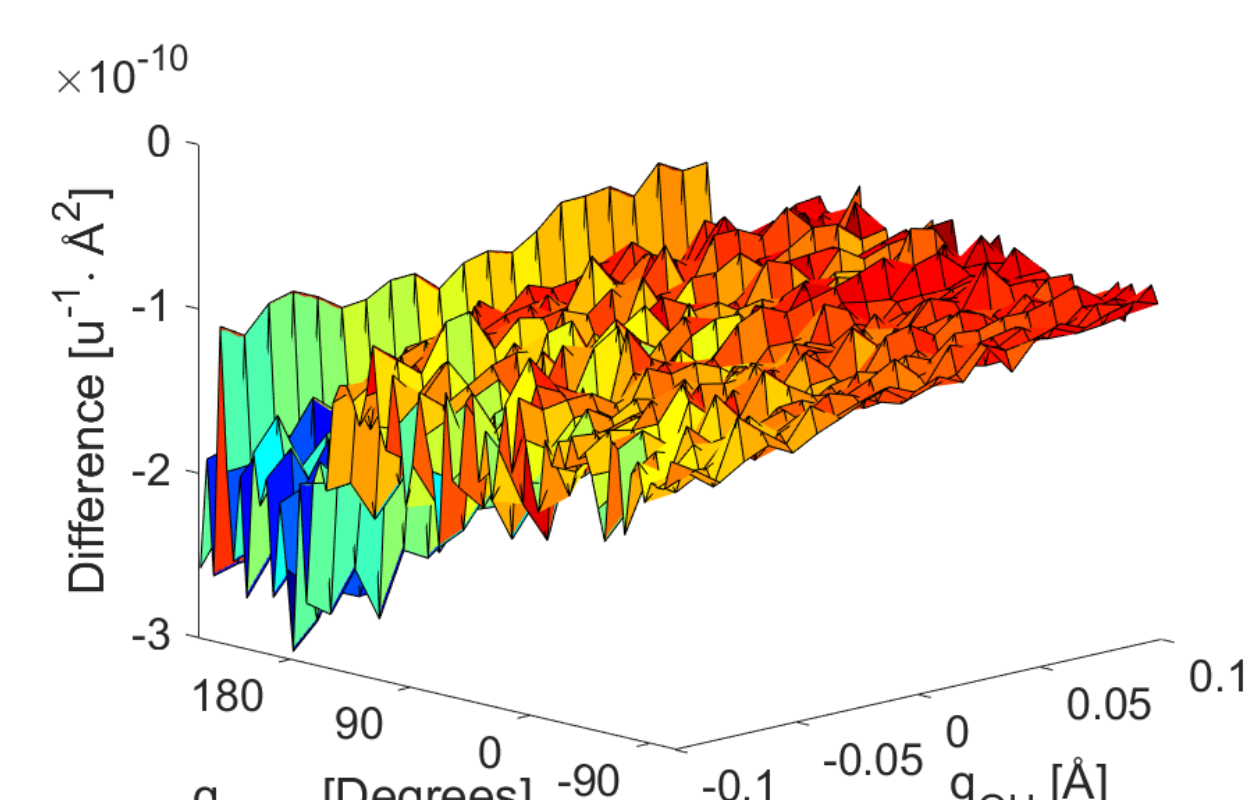


Figure 3: Difference between the numeric and analytical G-matrix element for the COH-bending mode in Gg-1-propanol. The difference is on the 11th digit.

In Figure 4, we compare calculated^[2] (3D LM) and experimental^[3] OH-stretching fundamental transition intensities for five alcohols (methanol, ethanol, 1-propanol, 2-propanol and *tert*-butanol). The three modes included in the LM model are the OH-stretching mode, the CO-stretching mode and the COH-bending mode. The PES's and DMF's were calculated with CCSD(T)-F12a/VDZ-F12 using MOLPRO 2012.1.

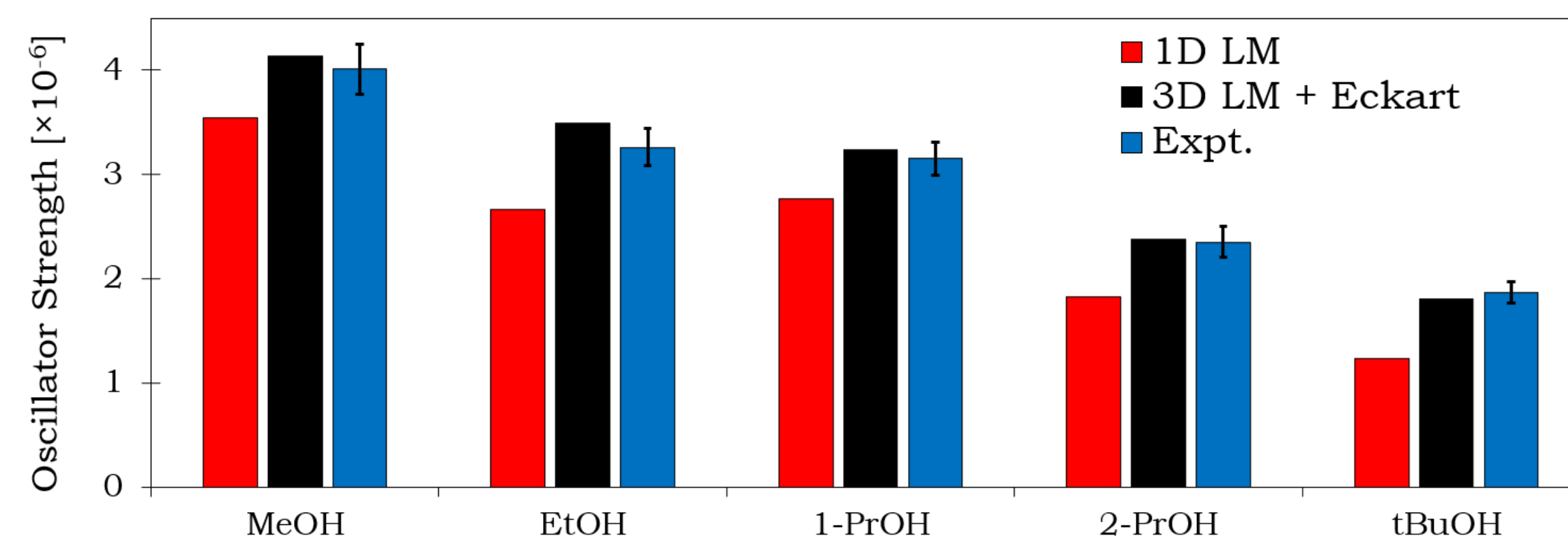


Figure 4: Calculated and experimental fundamental transition intensities.

1-propanol has five unique conformers that all contribute to the vibrational band profiles observed at room temperature (Figure 5). The calculated spectra includes no empirical parameters except for the line broadening, used in PGOPHER.

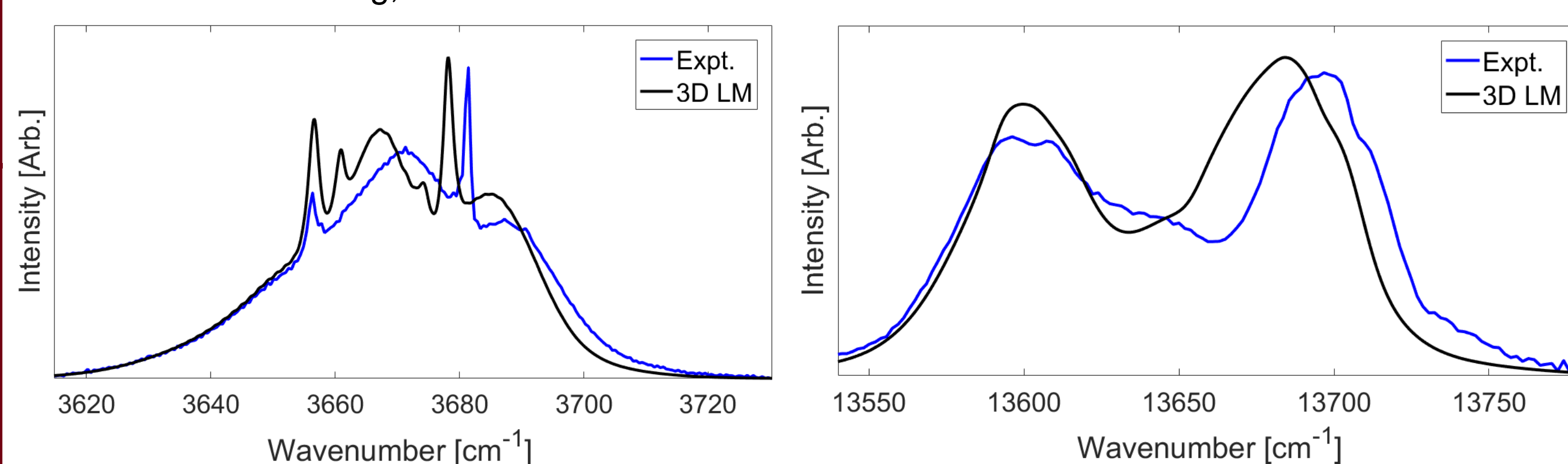


Figure 5: Calculated and experimental band profiles for the $\Delta\nu_{\text{OH}} = 1$ (left) and $\Delta\nu_{\text{OH}} = 4$ (right) region of 1-propanol. The calculated spectra are normalized to the calculated oscillator strengths, hence the experimental and calculated spectra can be compared in an absolute sense. PGOPHER is used to simulate the rotational fine structure.

Transition Intensities in Hydrogen Bond Complexes

When a bimolecular complex is formed, six new low-frequency intermolecular vibrations arise, due to the collective loss of three rotational and three translational degrees of freedom for the monomers. These intermolecular modes, illustrated in Figure 6 for the water dimer,^[4] significantly affect the OH-stretching mode directly involved in the hydrogen bond.^[5]

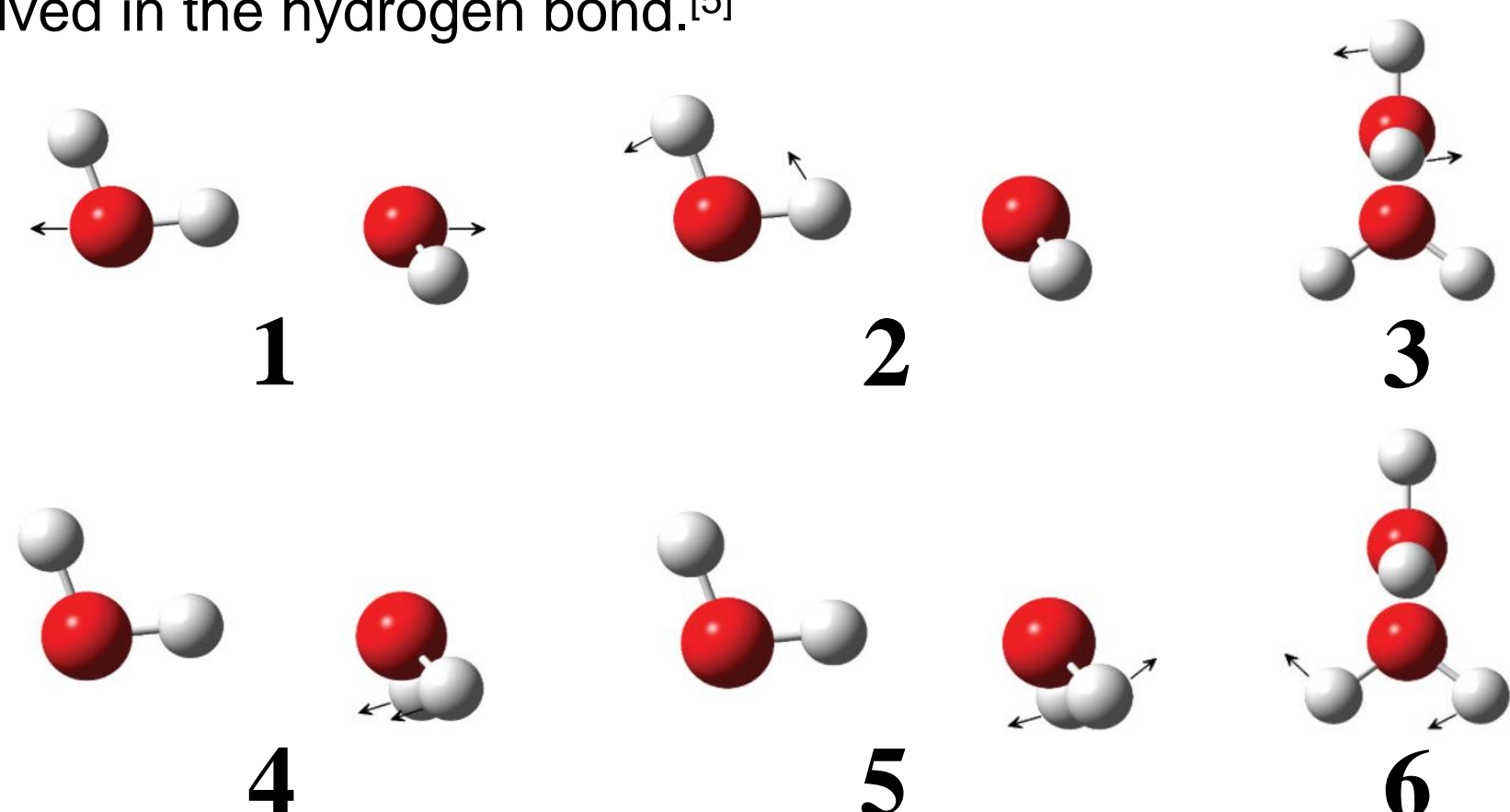


Figure 6: The six intermolecular modes of the water dimer. Mode (2) and (3) severely affect the bound OH-stretching oscillator by partially breaking the hydrogen bond for both positive and negative displacements.

In Figure 7, we show a room temperature fourier-transform infrared spectrum (FTIR) gas phase spectrum in the OH-stretching region of the water dimethylamine complex ($\text{H}_2\text{O} \cdot \text{DMA}$).

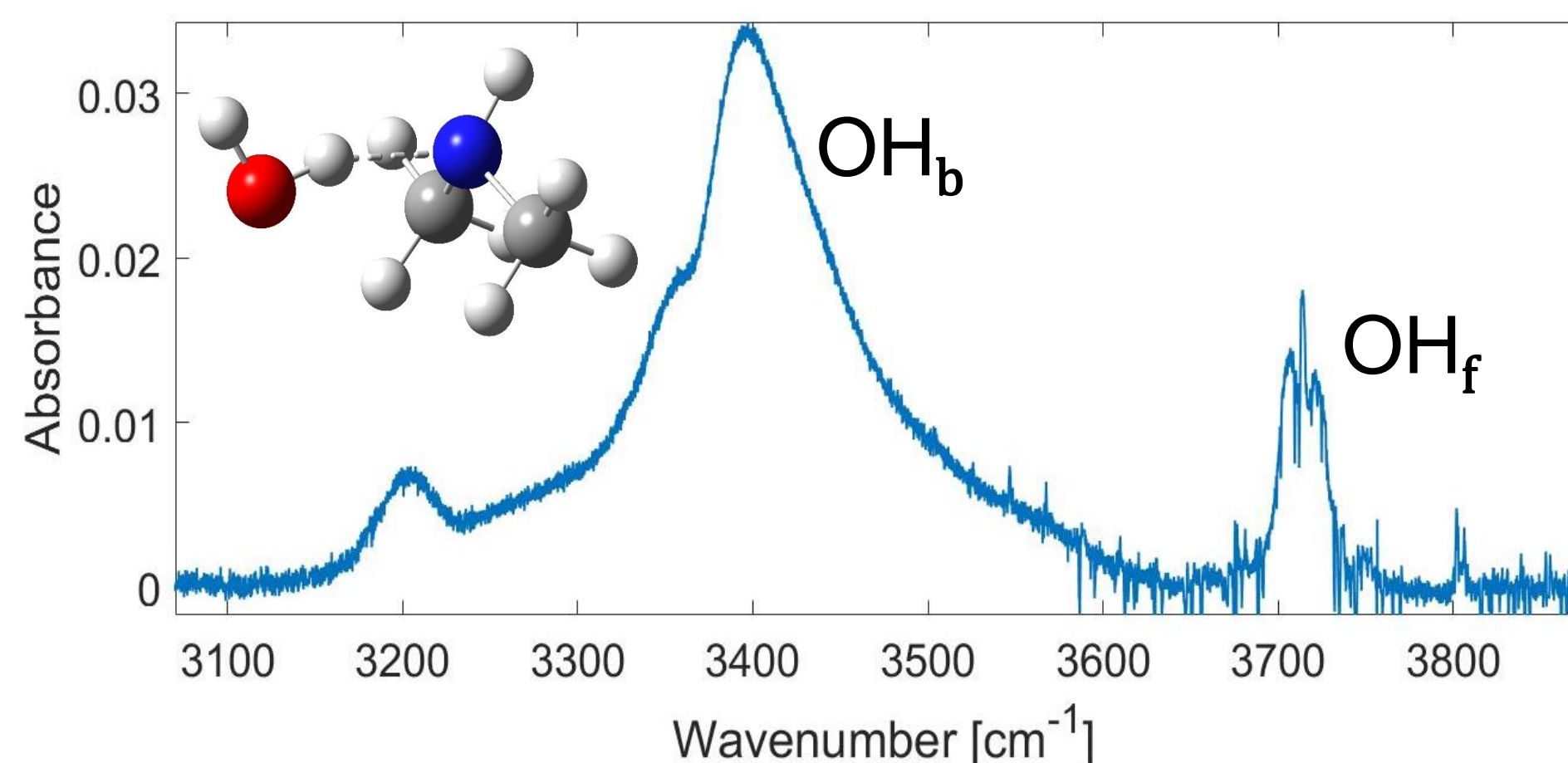


Figure 7: Room temperature gas phase FTIR spectrum in the OH-stretching region of $\text{H}_2\text{O} \cdot \text{DMA}$. The three bands are assigned as; the first HOH-bending overtone ($\sim 3200 \text{ cm}^{-1}$), the bound OH-stretching (OH_b) fundamental transition (middle) and the free OH-stretching (OH_f) fundamental transition (right).

The amount of a molecular complex in a gas mixture is proportional to the integrated absorbance ($\int A(\tilde{\nu}) d\tilde{\nu}$) of a transition unique to the complex, and inversely proportional to the corresponding oscillator strength (f),

$$P_{\text{Complex}} \propto \frac{\int A(\tilde{\nu}) d\tilde{\nu}}{f}. \quad (6)$$

The equilibrium constant of complex formation may be obtained if the oscillator strength and integrated absorbance of a transition unique to the complex is known, as well as the pressure of the monomers. The equilibrium constant is given by:

$$K = \frac{P_{\text{Complex}} \times P^\ominus}{P_{\text{H}_2\text{O}} \times P_{\text{DMA}}}, \quad (7)$$

where P^\ominus is the IUPAC standard pressure of 1 bar. We have used a 3D+6D LM model to calculate the oscillator strength (Eq. 6) for the free and bound OH-stretching fundamental transition in $\text{H}_2\text{O} \cdot \text{DMA}$. In Table 1, we show the equilibrium constant (Eq. 7) of complex formation obtained from the bound and free OH-stretching fundamental transition, respectively, at room temperature ($297 \pm 1 \text{ K}$).^[6]

$\text{H}_2\text{O} \cdot \text{DMA}$	OH_b	OH_f
$K(297 \pm 1 \text{ K})$	0.26 ± 0.06	0.23 ± 0.02

Table 1: Equilibrium constant of complex formation for $\text{H}_2\text{O} \cdot \text{DMA}$ at $297 \pm 1 \text{ K}$. The PES and DMF is calculated with CCSD(T)-F12a/VDZ-F12.

References

- [1] S. V. Krasnoshchekov *et al.* J. Chem. Phys. 140, 154104, 2014 | [2] E. Vogt, and H. G. Kjaergaard, Unpublished | [3] J. Wallberg *et al.* Spectrochim. Acta. A, 208, 315, 2019
 [4] K. Mackeprang *et al.* J. Chem. Phys. 140, 184309, 2014 | [5] A. S. Hansen, *et al.* Int. Rev. Phys. Chem. 38, 115, 2019 | [6] E. Vogt *et al.*, Unpublished